

# A catalogue of simulated jerks from a geodynamo model approaching Earth's core conditions

Julien Aubert

*4DEarth\_Swarm\_Core ESA project deliverable D-E.1*

---

## 1 General description

This document refers to publicly available output data from a geodynamo simulation that approaches closely to the physical conditions of Earth's core. In the model parameter space, this model is part of a series that defines a path connecting the conditions where classical dynamo models are found to those of the Earth's core. The theoretical definition of this path may be found in [Aubert et al. \(2017\)](#), and the model described here is located at 71% of this path (path parameter  $\epsilon = 10^{-5}$ ). This model is fully described in [Aubert & Gillet \(2021\)](#). Table 1 lists the key time scales and associated dimensionless numbers of this model together with those expected at Earth's core conditions.

From the dimensionless outputs of the numerical model, the provided data files are **already scaled to dimensional values**. Here I mention some details for the re-scaling procedure that has been applied. Re-scaling can be done in a completely self-consistent manner only once the model conditions reach those of the Earth's core. The path theory serves to rescale these quantities in a way that rationalizes the gap that still exists between those two conditions ([Aubert, 2018, 2020](#)). For the time series presented here, the time basis is provided by the choice of the magnetic diffusivity  $\eta$  in table 1. From there and the value of the magnetic Reynolds number  $Rm$  immediately follow the determination of the core overturn time  $\tau_U$  involving the root-mean-squared flow velocity  $U$  in the shell and the re-scaling of the velocity field. The value of the Lundquist number gives access to the Alfvén time  $\tau_A$ , which however differs from its target Earth value as we are not yet at the end of the path. The r.m.s dimensional magnetic field amplitude  $B$  can therefore be obtained by considering that the density  $\rho$  of the simulated fluid shell is  $(5.8/2)^2$  time stronger than its Earth counterpart  $\rho = 11000 \text{ kg/m}^3$ , this former factor accounting for the differences in the model and Earth Alfvén times. Finally, the density anomaly field is rescaled following [Aubert & Gillet \(2021\)](#), by expressing the dimensionless field in units of  $\rho\Omega\eta/g_oD$  (where  $g_o$  is the gravity at the core surface), and multiplying

3 March 2021

Quantity	Definition	71% of path model	Earth's core
Earth radius	$a$	6371.2 km	6371.2 km
core surface radius	$r_o$	3485 km	3485 km
outer core thickness	$D$	2260 km	2260 km
magnetic diffusivity	$\eta$	1.2 m <sup>2</sup> /s	$\approx 1.2$ m <sup>2</sup> /s
magnetic diffusion time	$\tau_\eta = D^2/\eta$	135000 yr	$\approx 135000$ yr
planetary rotation period	$2\pi\tau_\Omega = 2\pi/\Omega$	12 days	1 day
Alfvén time	$\tau_A = \sqrt{\rho\mu}D/B$	5.8 yr	$\approx 2$ yr
1D Alfvén speed	$D/\sqrt{3}\tau_A$	225 km/yr	$\approx 650$ km/yr
core overturn time	$\tau_U = D/U$	118 yr	$\approx 120$ yr
1D convective speed	$D/\sqrt{3}\tau_U$	11 km/yr	$\approx 11$ km/yr
Magnetic Ekman number	$E/Pm = \tau_\Omega/\tau_\eta$	$3.8 \cdot 10^{-8}$	$\approx 3.2 \cdot 10^{-9}$
Magnetic Reynolds number	$Rm = \tau_\eta/\tau_U$	1140	$\approx 1100$
Lundquist number	$S = \tau_\eta/\tau_A$	23300	$\approx 68000$

Table 1

Key parameters for the model, presented together with their model values and values expected at Earth's core conditions.  $B$  and  $U$  are root-mean-squared amplitudes of the magnetic field inside the simulated core.

the result with Earth's core dimensional estimate for  $\rho\Omega\eta/g_oD$  obtained with  $g_o = 10$  m/s<sup>2</sup>,  $\rho = 11000$  kg/m<sup>3</sup> and the other values from Table 1.

Figure 1 presents temporal sequences of the core-mantle boundary secular acceleration energy (as defined in [Aubert, 2018](#)) and Earth-surface jerk energy (as defined in [Aubert & Finlay, 2019](#)). The outputs that are made available here specifically focus on the 14 simulated geomagnetic jerk events marked with arrows in Figure 1. These outputs first consist in high-resolution time series of the coefficients describing the poloidal magnetic field outside the core and the velocity field at the core surface. The time series cover a few decades before and after the approximate timestamps of jerks presented in Table 2. Their temporal resolution is set to 0.05 years i.e. four times finer than the long time series covering the entire sequence that were previously provided in deliverable D-C.1. The model operates with stress-free boundary conditions, which implies that Ekman boundary layers are not described and that the core surface directly corresponds to the free stream. For each jerk event, a collection of movies representing these time series is also provided. Finally, full three-dimensional states of the simulation at selected times are provided for a selection of jerks.

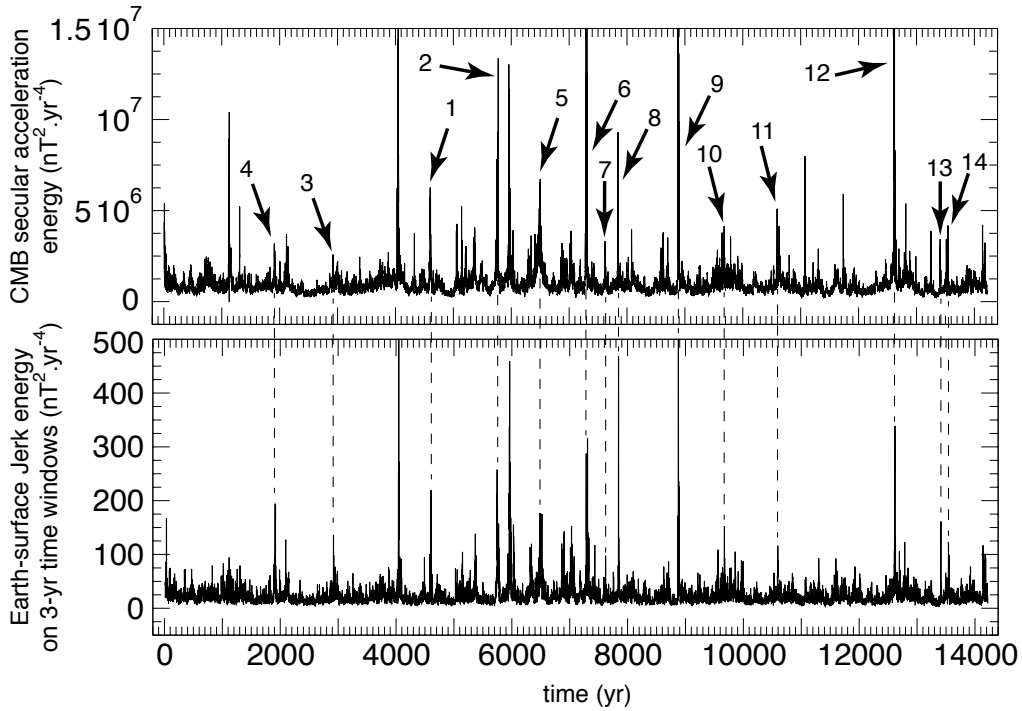


Fig. 1. Core-mantle boundary (CMB) secular acceleration energy (top) and Earth-surface jerk energy (bottom), as functions of the dimensional simulation time. See [Aubert \(2018\)](#); [Aubert & Finlay \(2019\)](#) for definitions. Following these references, the outputs on this figure have been truncated at spherical harmonic degree and order 13, but the publicly available outputs are supplied up to a higher spherical harmonic resolution of 30.

Jerk No.	timestamp (years)	Jerk No.	timestamp (years)
1	4600	8	7840
2	5750	9	8880
3	2920	10	9673
4	1915	11	10590
5	6490	12	12620
6	7300	13	13411
7	7620	14	13546

Table 2

Approximate timestamps for simulated jerks in the catalogue.

## 2 Data format and description

### 2.1 Magnetic field coefficients

To describe the magnetic field at and above the core surface, we adopt the classical Gauss coefficient description for the magnetic field. Denoting the colatitude as  $\theta$  and the Greenwich-centered longitude as  $\varphi$ , the poloidal field at a radius  $r$  above the core-mantle boundary may be written

$$\mathbf{B}_p(r, \theta, \varphi, t) = -\nabla V \quad (1)$$

where

$$V(r, \theta, \varphi, t) = a \sum_{l=1}^{30} \left(\frac{a}{r}\right)^{l+1} \sum_{m=0}^l [g_l^m(t) \cos m\varphi + h_l^m(t) \sin m\varphi] P_l^m(\cos \theta). \quad (2)$$

Here  $t$  is time,  $a = 6371.2$  km is Earth's magnetic radius of reference,  $P_l^m$  is the Schmidt-seminormalised Legendre function of degree  $l$  and order  $m$ .

For each jerk event, the file `Gauss_Bsurf.mat` (MATLAB data format) comprises the dimensional timestamp vector `timers` (in years) containing the discrete values of  $t$  and an array `gnm` containing the coefficients  $g_l^m(t)$ ,  $h_l^m(t)$  (in nanoteslas) arranged according to:

$$\begin{aligned} \text{gnm}(:, 1) &= g_1^0(t) \\ \text{gnm}(:, 2) &= g_1^1(t) \\ \text{gnm}(:, 3) &= h_1^1(t) \\ \text{gnm}(:, 4) &= g_2^0(t) \\ \text{gnm}(:, 5) &= g_2^1(t) \\ \text{gnm}(:, 6) &= h_2^1(t) \\ \text{gnm}(:, 7) &= g_2^2(t) \\ \text{gnm}(:, 8) &= h_2^2(t) \\ &\dots \\ \text{gnm}(:, 959) &= g_{30}^{30}(t) \\ \text{gnm}(:, 960) &= h_{30}^{30}(t) \end{aligned}$$

Note that the sinus coefficients corresponding to  $m = 0$  are not stored as they vanish identically. There are therefore 960 coefficients corresponding to a description of the output up to spherical harmonic degree and order 30. The core surface poloidal magnetic field is then obtained by setting  $r$  to  $r_o = 3485$  km in equation (2).

## 2.2 Velocity field coefficients

The core surface velocity field coefficients are described using the spheroidal-toroidal formalism. The  $\theta$  and  $\varphi$  components of the core surface velocity vector  $\mathbf{u}$  are written

$$\mathbf{u} = \begin{pmatrix} u_\theta = \frac{1}{\sin \theta} \frac{\partial T}{\partial \varphi} + \frac{\partial S}{\partial \theta} \\ u_\varphi = -\frac{\partial T}{\partial \theta} + \frac{1}{\sin \theta} \frac{\partial S}{\partial \varphi} \end{pmatrix} \quad (3)$$

The spectral decomposition of  $T$ ,  $S$  obeys

$$T = \sum_{l=1}^{30} \sum_{m=0}^l [tc_l^m(t) \cos m\varphi + ts_l^m(t) \sin m\varphi] P_l^m(\cos \theta) \quad (4)$$

$$S = \sum_{l=1}^{30} \sum_{m=0}^l [sc_l^m(t) \cos m\varphi + ss_l^m(t) \sin m\varphi] P_l^m(\cos \theta) \quad (5)$$

For each jerk event, the file `Gauss_Vsurf.mat` (MATLAB data format) contains the timestamp `timers` (in years) together with two arrays `tnm` and `snm` (in km.rad/yr) where the coefficients  $tc_l^m, ts_l^m$  and  $sc_l^m, ss_l^m$  are respectively stored. The ordering follows that of the magnetic field Gauss coefficients i.e.

$$\begin{aligned} \text{tnm}(:, 1) &= tc_1^0(t) \\ \text{tnm}(:, 2) &= tc_1^1(t) \\ \text{tnm}(:, 3) &= ts_1^1(t) \\ \text{tnm}(:, 4) &= tc_2^0(t) \\ \text{tnm}(:, 5) &= tc_2^1(t) \\ \text{tnm}(:, 6) &= ts_2^1(t) \\ \text{tnm}(:, 7) &= tc_2^2(t) \\ \text{tnm}(:, 8) &= ts_2^2(t) \\ &\dots \\ \text{tnm}(:, 959) &= tc_{30}^{30}(t) \\ \text{tnm}(:, 960) &= ts_{30}^{30}(t) \end{aligned}$$

Note that the sinus coefficients corresponding to  $m = 0$  are not stored as they vanish identically. As for the magnetic field coefficients above there are 960 coefficients for each scalar, corresponding to a description of the output up to spherical harmonic degree and order 30.

### 2.3 Movies

For each jerk event, a .zip archive is provided that contains the following mp4 movie files:

- `Brcmb.mov` and `Brcmb13.mov`: core surface radial magnetic field (in mT), respectively at native (up to spherical harmonic degree 170) and truncated (up to spherical harmonic degree 13) resolutions,
- `Vpcmb.mov`: core surface azimuthal velocity field (in km/yr) at native resolution,
- `dVcmb.mov`: core surface azimuthal velocity acceleration (in km/yr<sup>2</sup>) at native resolution,
- `SVcmb.mov`: core surface radial secular variation (first time derivative of the magnetic field, in  $\mu\text{T}/\text{yr}$ ) up to spherical harmonic degree 13,
- `SACmb.mov` and `SAsurf.mov`: core surface and Earth surface radial secular acceleration (second time derivative of the magnetic field, in nT/yr<sup>2</sup>) up to spherical harmonic degree 13.

### 2.4 Full three-dimensional states

For jerks 1,3 and 9, two states of the simulations at native spatial resolution are provided as (very large) binary files `Gt1` and `Gt2`. The two states are closely spaced in time such that a time derivative can be reliably computed. The states can be loaded into computer memory by using the provided matlab script `parodyload_scaled.m`.

Once loaded, the following variables are present in MATLAB memory:

- the dimensional timestamp `timers` (in years),
- the numbers of grid points `nr=1248` in radius, `nt=256` in latitude and `np=512` in longitude, with longitude `np=1` referring to 180 degrees East in the Pacific.
- the vectors `r(1:nr)` of radii within the outer core (in km), `theta(1:nt)` of colatitudes and `phi(1:np)` of longitudes (both in radians) defining the spherical coordinate frame,
- the three `(1:np, 1:nt, 1:nr)` arrays `Vr`, `Vt`, `Vp` of the outer core velocity field components (in km/yr),
- the three `(1:np, 1:nt, 1:nr)` arrays `Br`, `Bt`, `Bp` of the outer core magnetic field components (in mT),
- the `(1:np, 1:nt, 1:nr)` array `T` of the outer core scalar density anomaly field (in kg/m<sup>3</sup>). Note that this latter quantity is relative i.e. it can be shifted by an arbitrary constant (only the gradients matter).

## References

- Aubert, J., 2018. Geomagnetic acceleration and rapid hydromagnetic wave dynamics in advanced numerical simulations of the geodynamo, *Geophys. J. Int.*, **214**(1), 531–547.
- Aubert, J., 2020. Recent geomagnetic variations and the force balance in Earth's core, *Geophys. J. Int.*, doi: 10.1093/gji/ggaa007.
- Aubert, J. & Finlay, C. C., 2019. Geomagnetic jerks and rapid hydromagnetic waves focusing at Earth's core surface, *Nature Geosci.*, **12**(5), 393–398.
- Aubert, J. & Gillet, N., 2021. The interplay of fast waves and slow convection in geodynamo simulations nearing Earth's core conditions, *Geophys. J. Int.*, doi: 10.1093/gji/ggab054.
- Aubert, J., Gastine, T., & Fournier, A., 2017. Spherical convective dynamos in the rapidly rotating asymptotic regime, *J. Fluid. Mech.*, **813**, 558–593.